Electronic Supplementary Material (ESI) for Chemical Science.

Supporting Information

Auto-Controlled Fabrication of Metal-Porphyrin Framework Thin Film with Tunable Optical Limiting Effect

De-Jing Li,[ab] Zhi-Gang Gu*[a] and Jian Zhang*[a]

[a] State Key Laboratory of Structural Chemistry, Fujian Institute of Research on the Structure of Matter, Chinese Academy of Sciences, Fuzhou, Fujian 350002, P.R. China.

[b] University of Chinese Academy of Sciences, Beijing 100049, P.R. China.

Address correspondence to zggu@fjirsm.ac.cn and zhj@fjirsm.ac.cn

Table of content

Figure S13. The photocurrent response of PIZA-1 and C_{60}@PIZA-1 thin film with 10 cycles.

Figure S14. The current–voltage curve of PIZA-1 and C_{60}@PIZA-1 thin film with 10 cycles.

Figure S15. The XRD of C_{60}@PIZA-1 thin film prepared by the autoarm immersion method.

Figure S16. The IR of PIZA-1 thin film, C_{60}@PIZA-1 thin film and C_{60}.

Figure S17. The SEM image of C_{60}@PIZA-1 thin film prepared by using the autoarm immersion method.

Figure S18. The NLO behavior of the C_{60}@PIZA-1 thin film at the different incident pulse energy.

Figure S19. The NLO behavior of the porphyrin ligand, C_{60} and porphyrin ligand mixed with C_{60} film quartz glass at 100 μJ.

Figure S20. The thicknesses of porphyrin ligand, C_{60} and the porphyrin ligand mixed with C_{60} film on quartz glass.

Figure S21. The curves of output fluence versus input fluence for bare glass, PIZA-1 thin film and C_{60}@PIZA-1 thin film.

Figure S22. The fluorescence spectra of PIZA-1 and C_{60}@PIZA-1 thin film.

Figure S23. The EIS curves of C_{60}@PIZA-1 thin film with and without laser irradiation.

Table S2. Comparison of band gap of porphyrin-fullerene systems

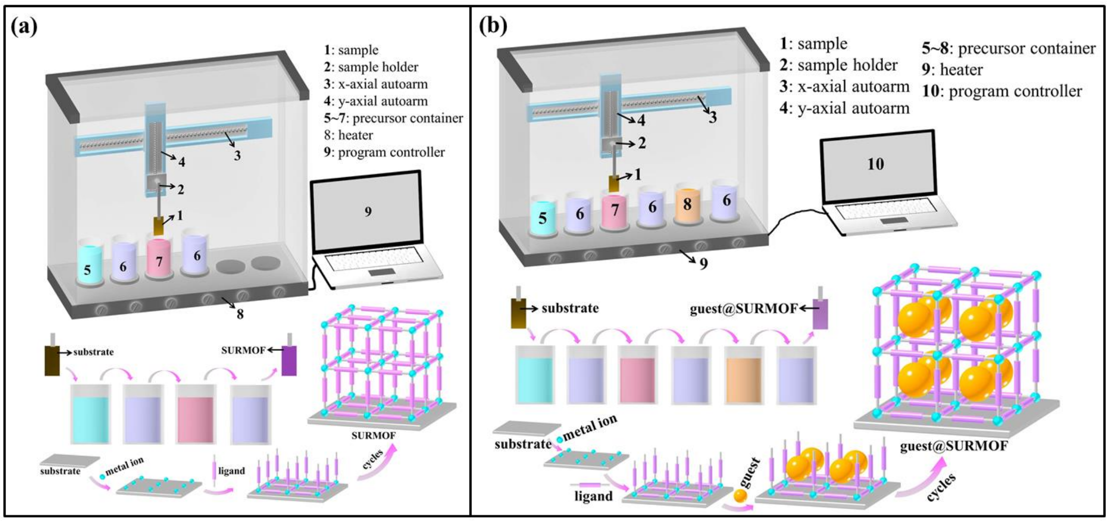

Figure S1. The scheme illustration of the preparation process of SURMOF (a) and guest@SURMOF (b) by the autoarm immersion method.

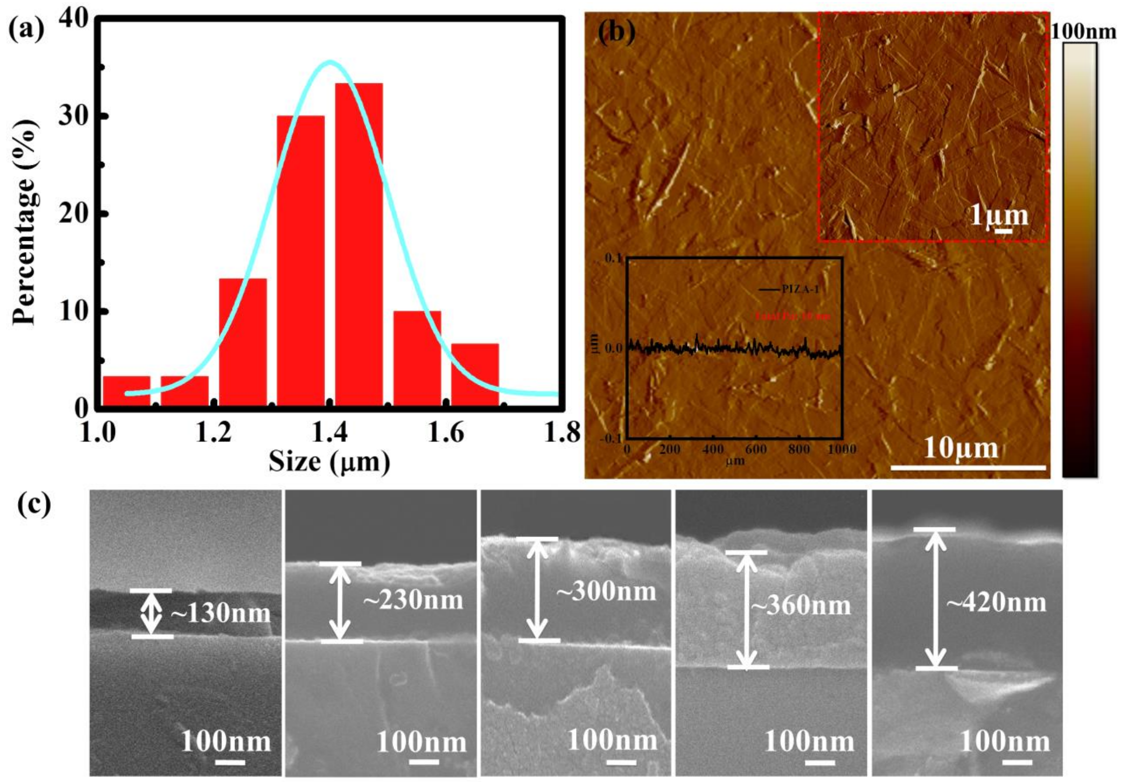

Figure S2. (a) The distribution curves of the domain width size for PIZA-1 thin film (b) The AFM images of PIZA-1 thin film (inset: The surface roughness of PIZA-1 thin film) (c) The cross-sectional SEM images of PIZA-1 thin film with different cycles of 5 cycles, 10 cycles, 15 cycles, 20 cycles, 25 cycles.

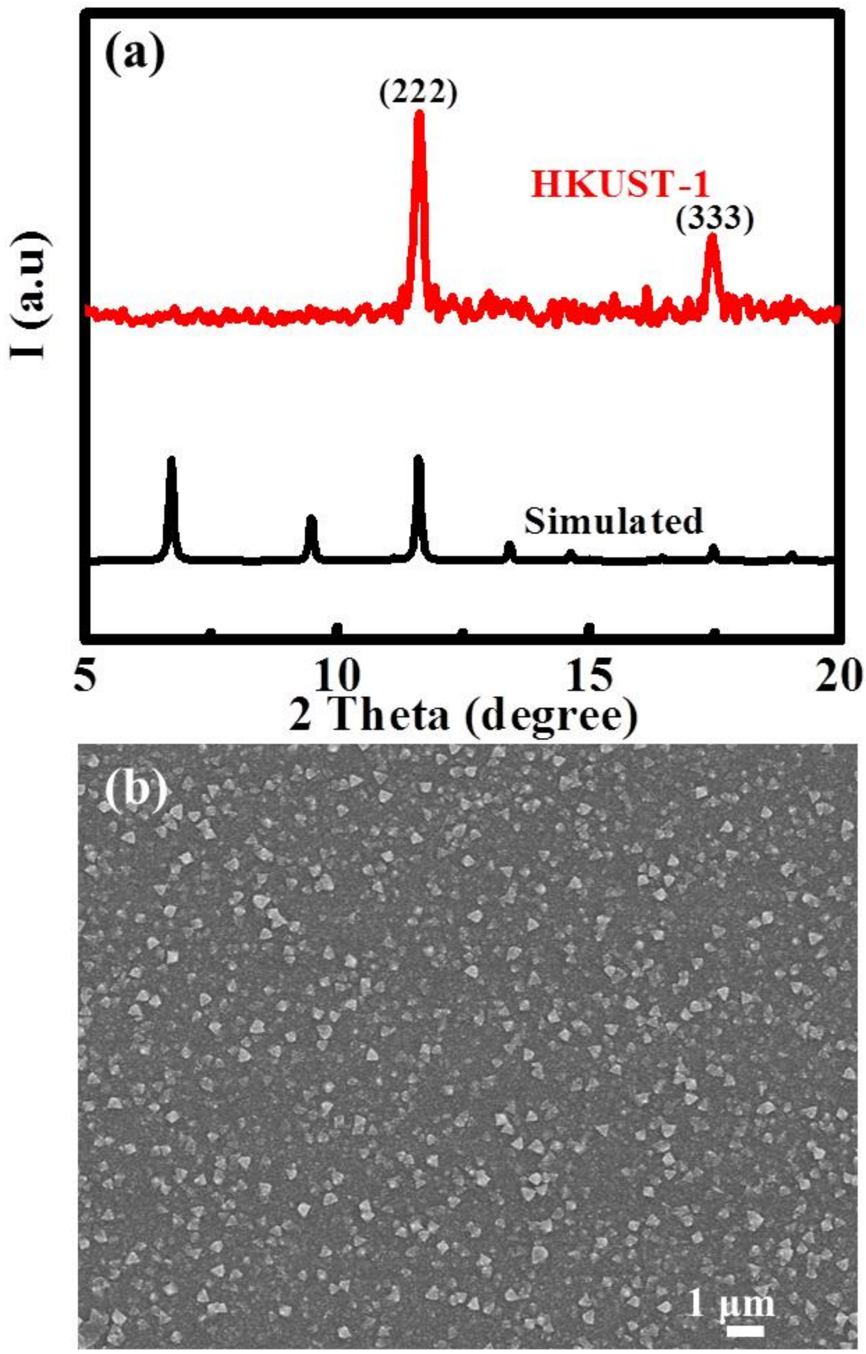

Figure S3. The XRD (a) and surface SEM images (b) of HKUST-1 thin film prepared by the autoarm immersion method.

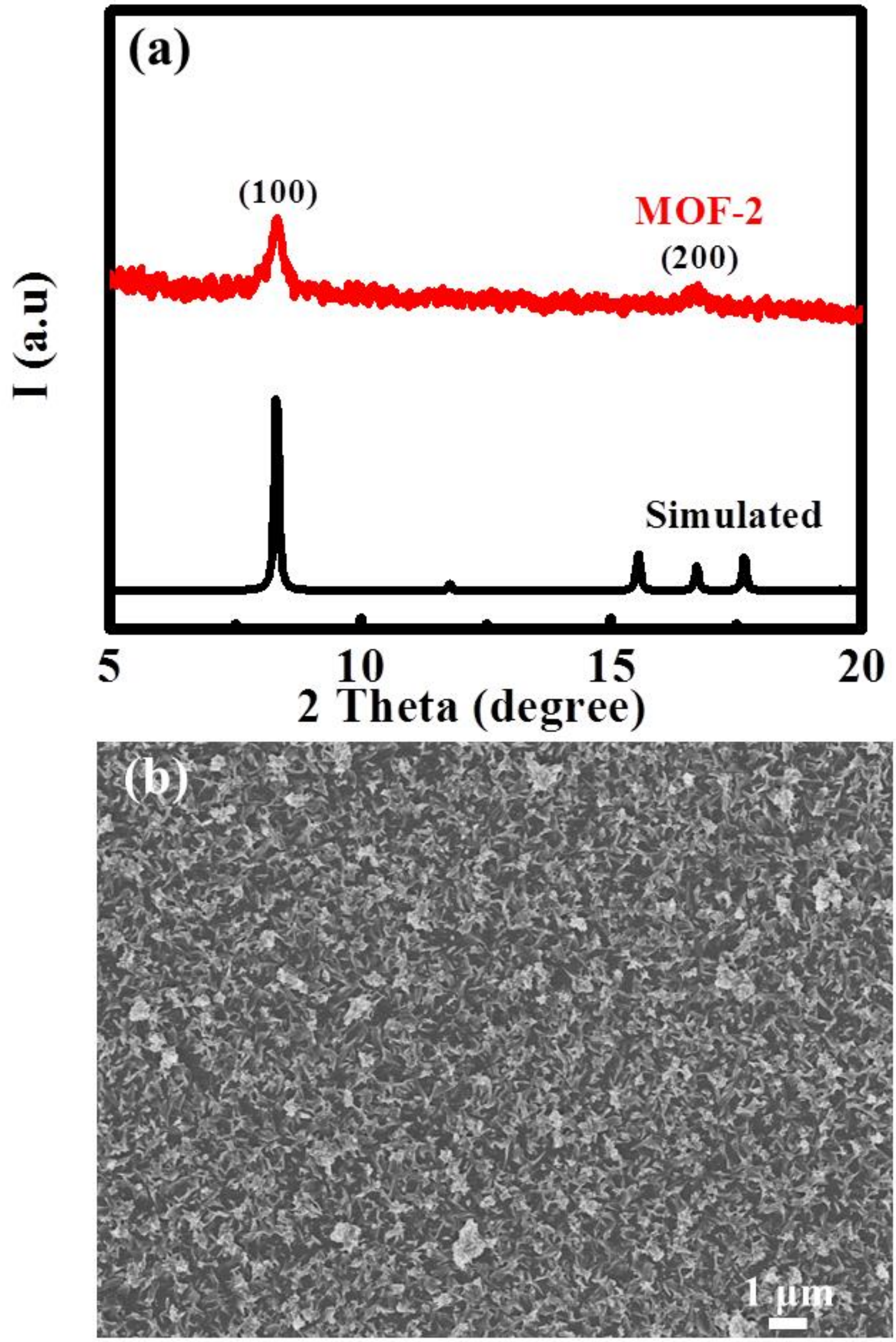

Figure S4. The XRD (a) and surface SEM images (b) of MOF-2 thin film prepared by the autoarm immersion method.

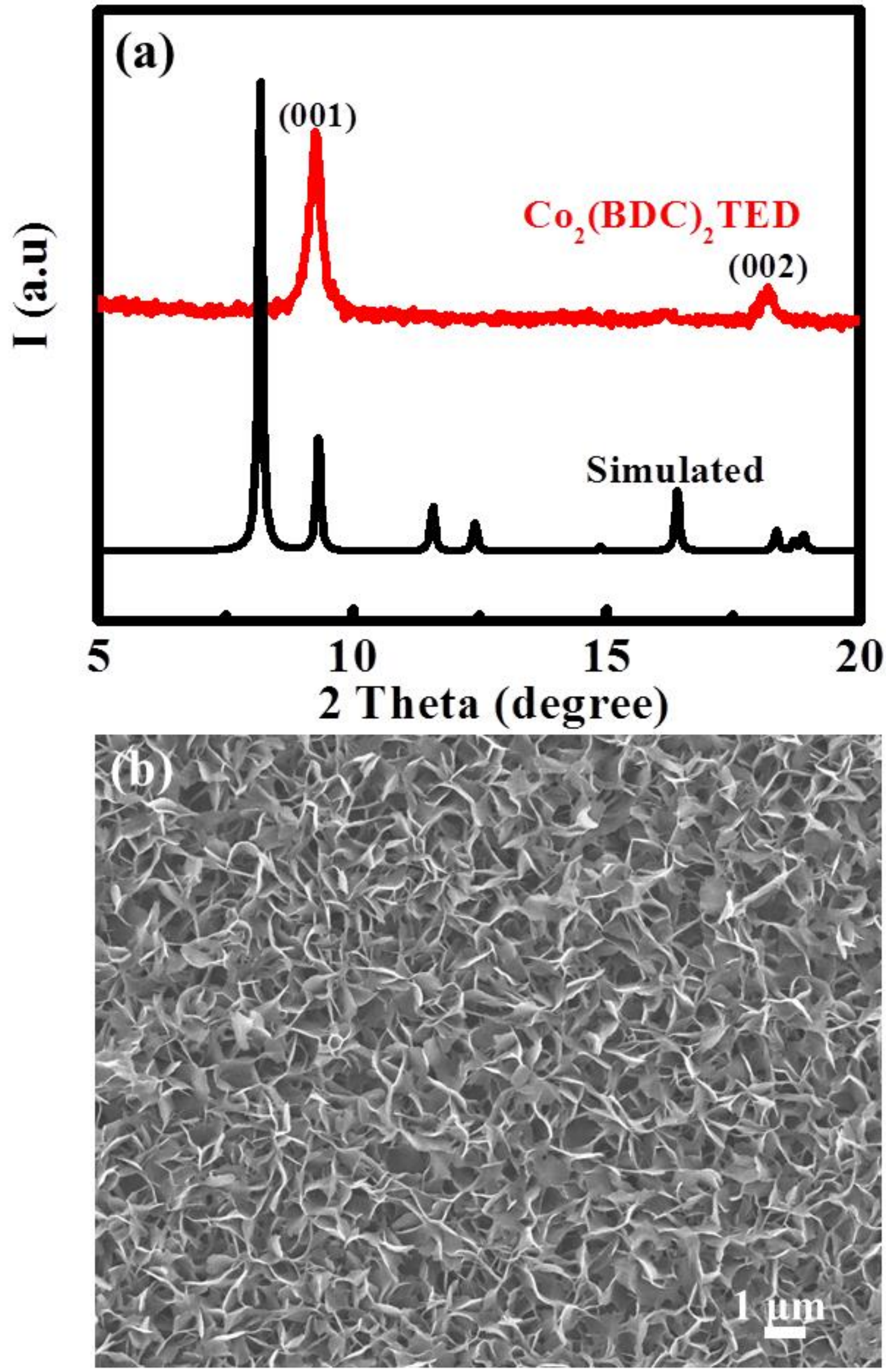

Figure S5. The XRD and surface SEM images of $Co_2(BDC)_2TED$ thin film prepared by the autoarm immersion method.

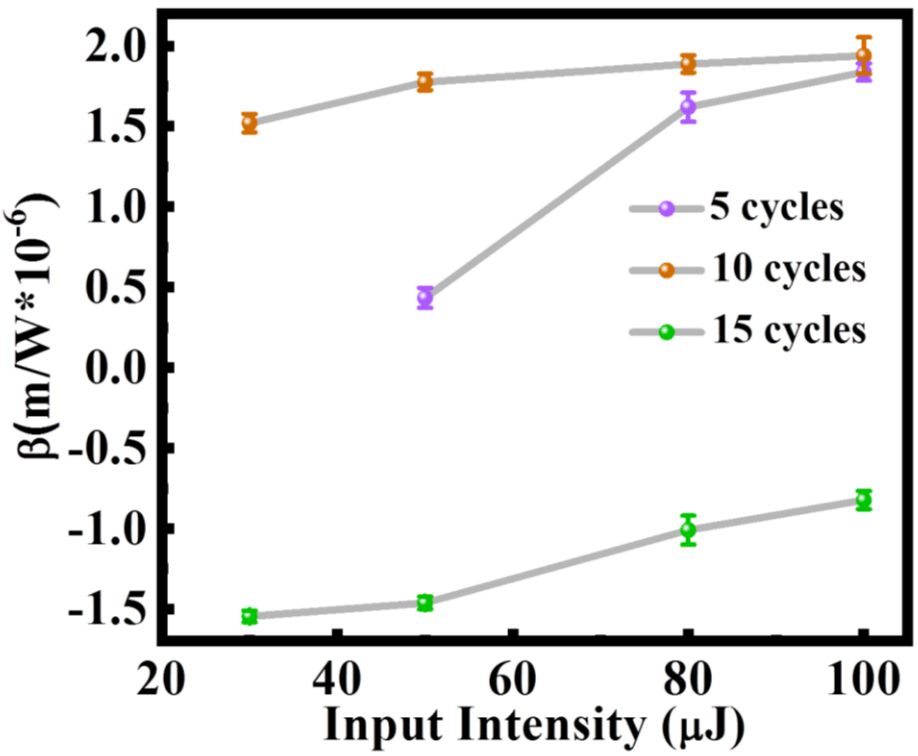

Figure S6. The nonlinear absorption coefficient of PIZA-1 thin film with different thickness versus different incident pulse energy.

Table S1. Linear and NLO data of the samples. E: incident pulse energy; T_0: linear transmittance; β: nonlinear coefficient.

sample	E (μJ)	T_0(%)	T_{min}	β(×10^{-6} m/W)
PIZA-1-5	30	95	1	--
	50	96	0.96	0.42
	80	94	0.81	1.70
	100	94	0.74	1.85
PIZA-1-10	30	88	0.87	1.50
	50	88	0.78	1.80
	80	87	0.70	1.87
	100	86	0.65	1.90
PIZA-1-25	30	35	1.26	-1.55
	50	35	1.79	-1.48
	80	35	2.07	-1.00
	100	34	2.27	-0.84

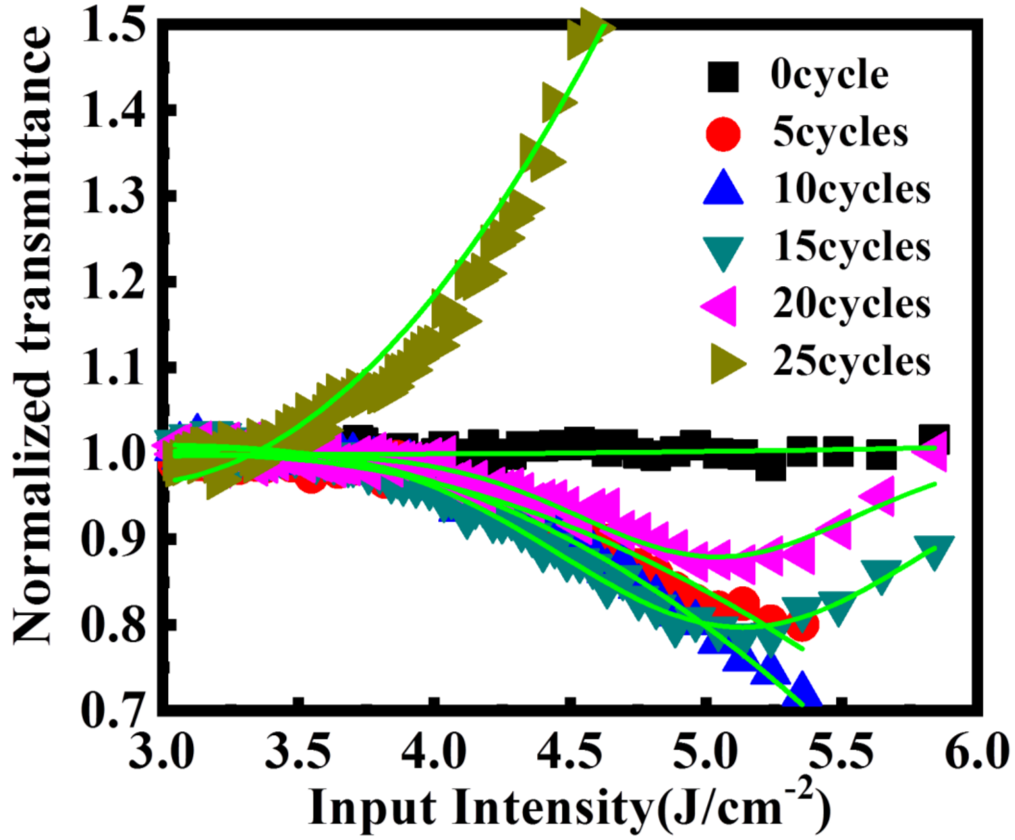

Figure S7. The normalized transmittance of PIZA-1 thin film with different thickness as a function of input intensity.

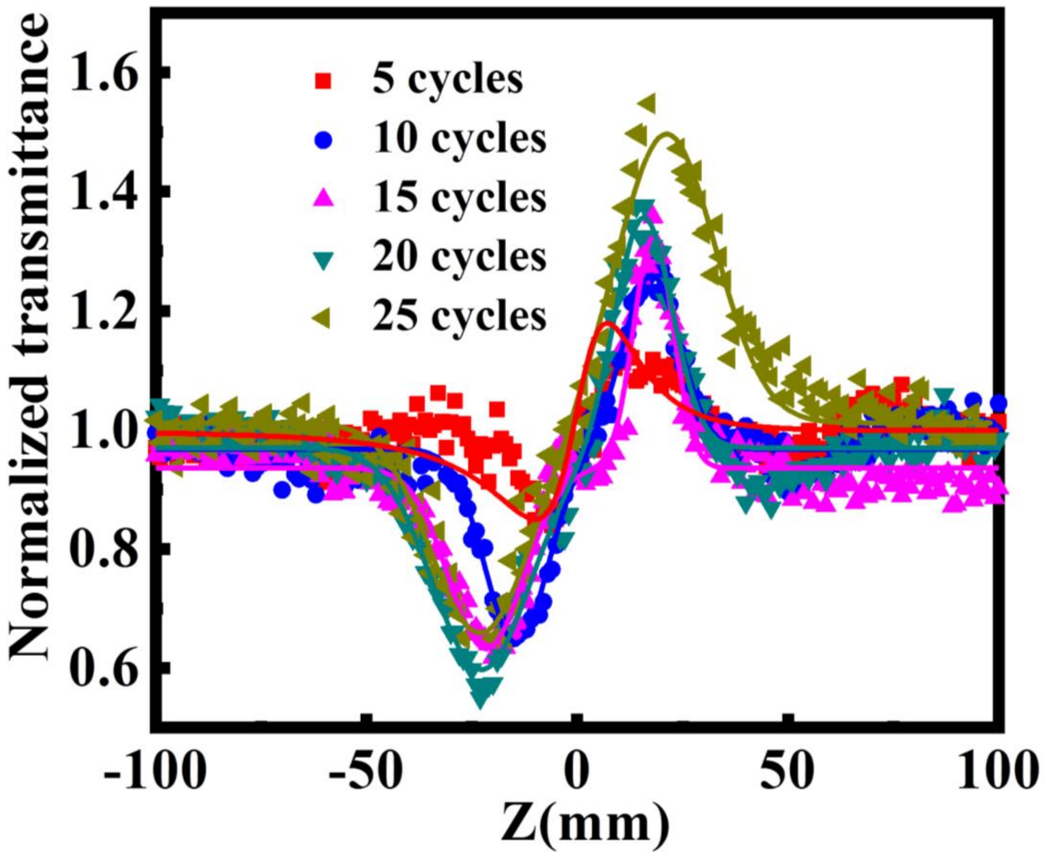

Figure S8. The nonlinear refraction response of PIZA-1 thin film with different thickness at the incident pulse energy of 100 μJ.

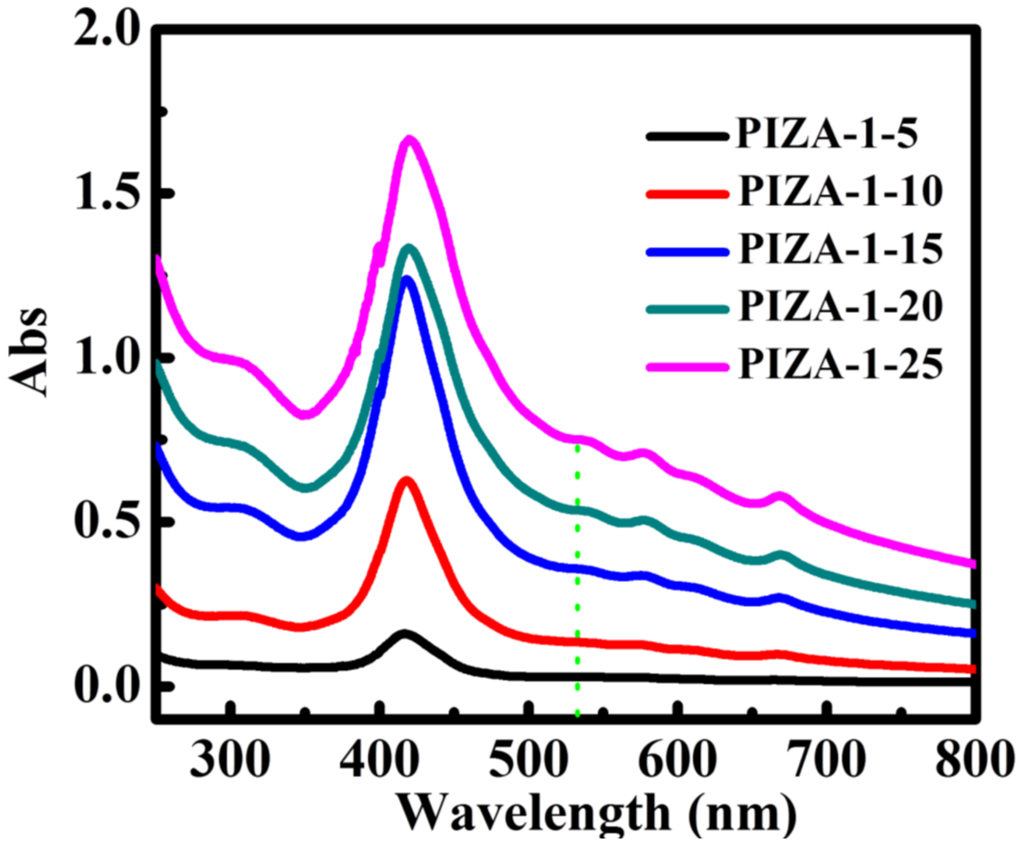

Figure S9. The UV-vis absorbance spectra of PIZA-1 thin film with different thickness.

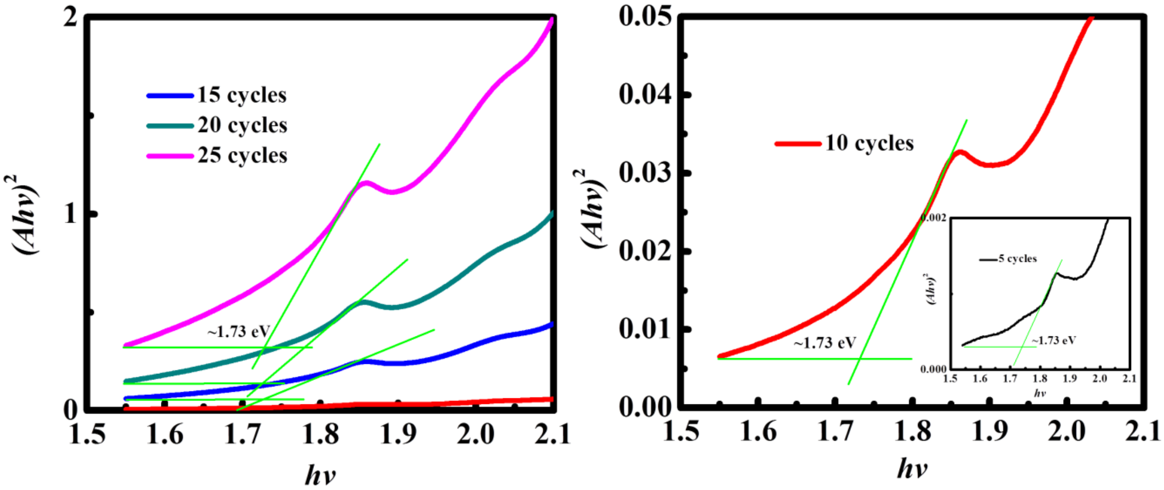

Figure S10. The diagram used to calculate the band gap of the PIZA-1 thin film with different thickness.

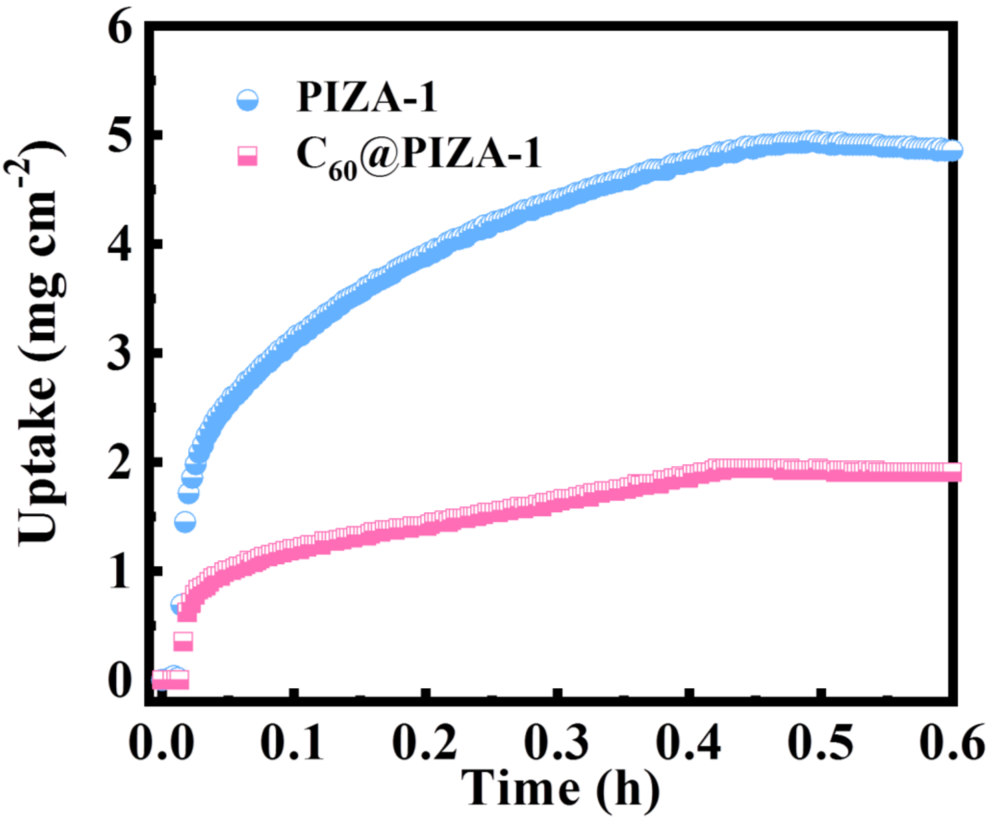

Figure S11. The mass uptakes of water for PIZA-1 and C_{60}@PIZA-1 thin film with 10 cycles.

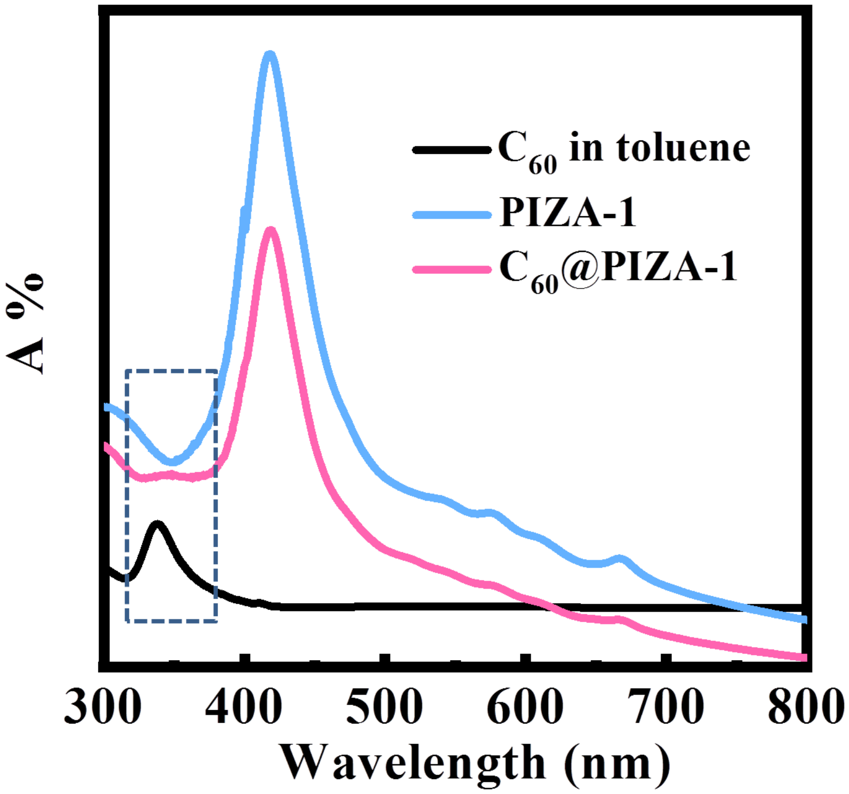

Figure S12. The UV-vis absorbance spectra of PIZA-1, C_{60}@PIZA-1 thin film with 10 cycles and C_{60} in toluene.

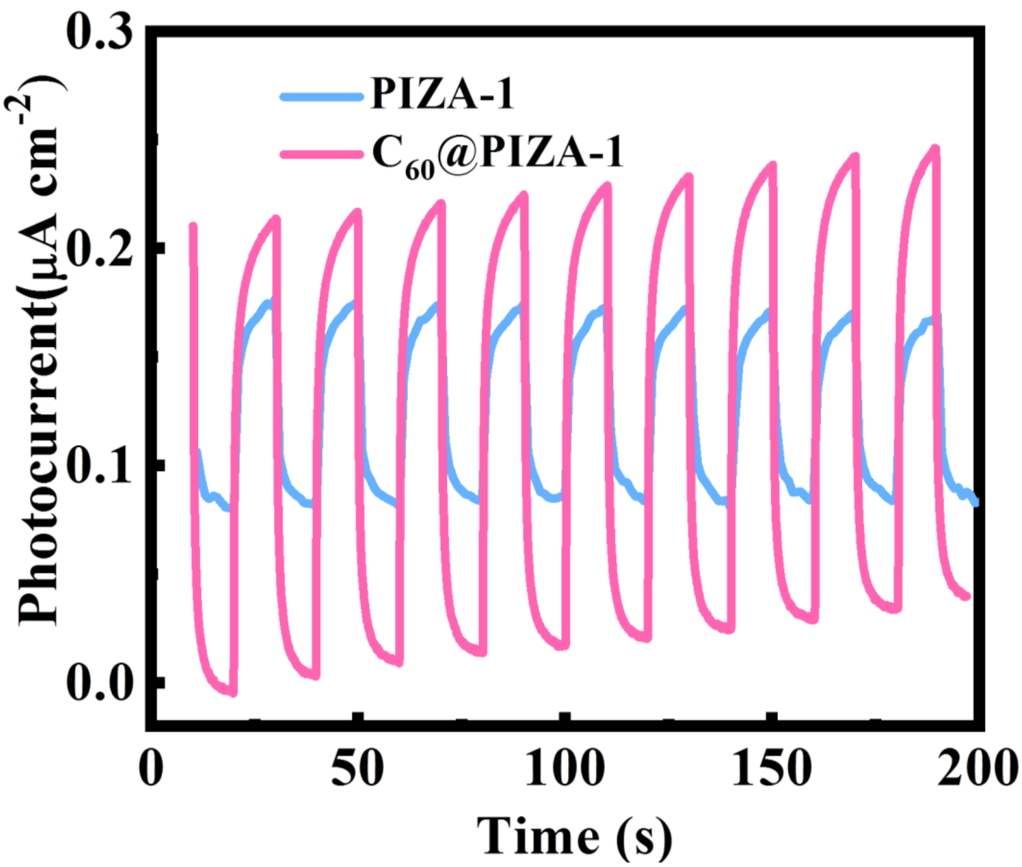

Figure S13. The photocurrent response of PIZA-1 and C_{60}@PIZA-1 thin film with 10 cycles.

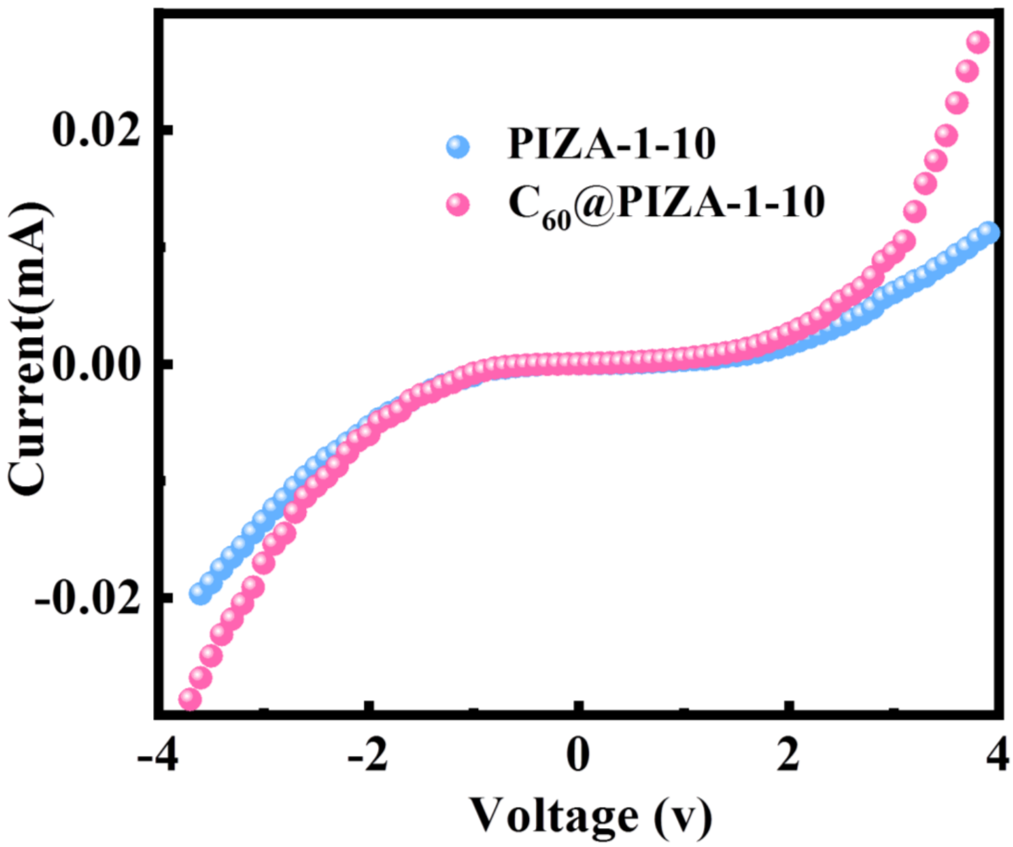

Figure S14. The current–voltage curve of PIZA-1 thin film and C_{60}@PIZA-1 thin film with 10 cycles.

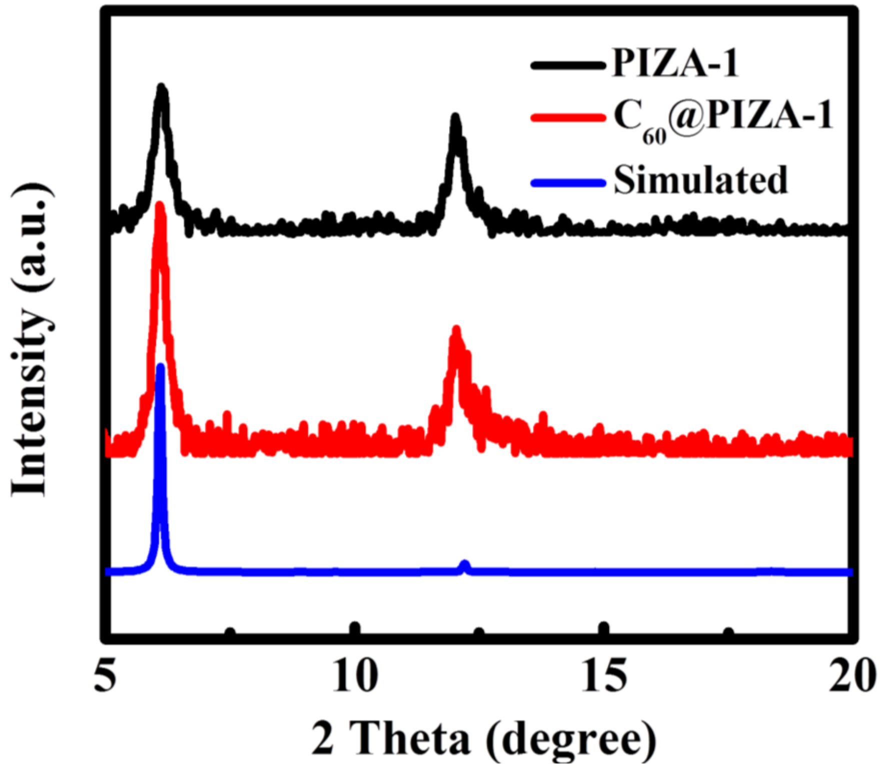

Figure S15. The XRD of C_{60}@PIZA-1 thin film prepared by using the autoarm immersion method.

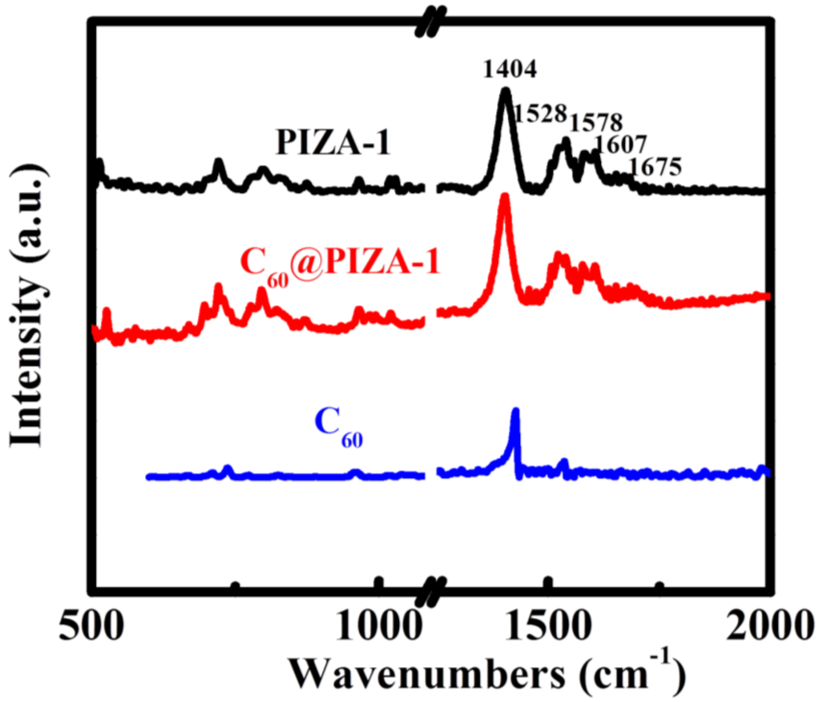

Figure S16. The IR of PIZA-1 thin film, C_{60}@PIZA-1 thin film and C_{60}.

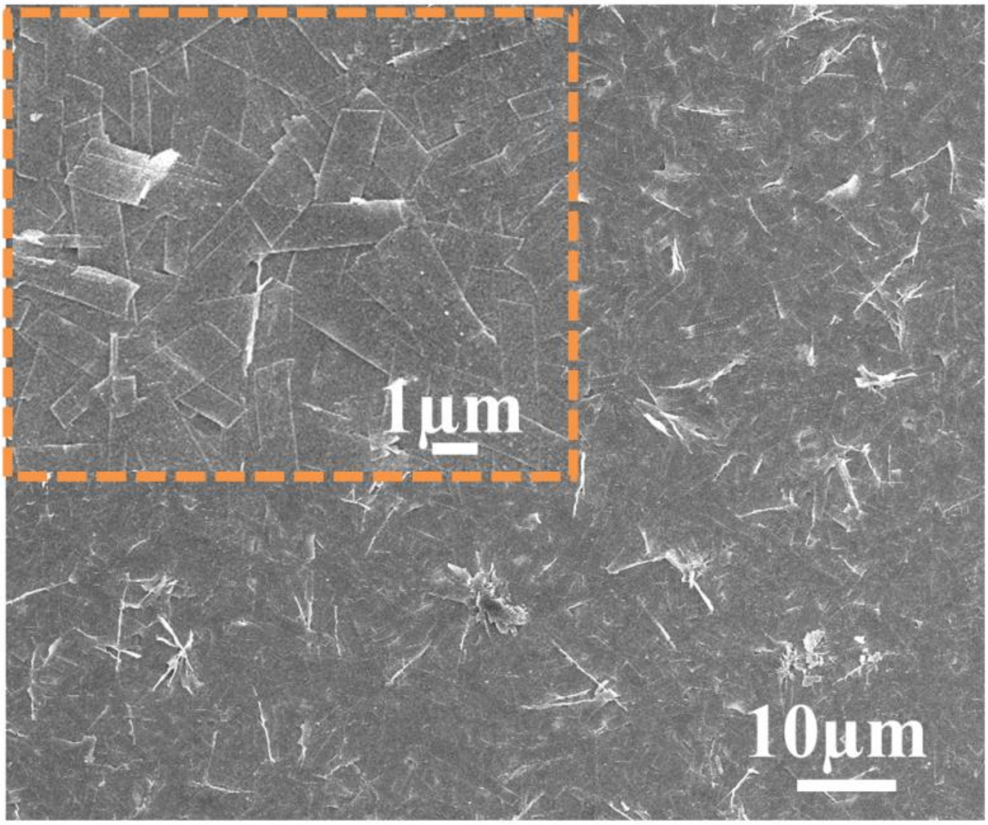

Figure S17. The SEM image of C_{60}@PIZA-1 thin film prepared by using the autoarm immersion method.

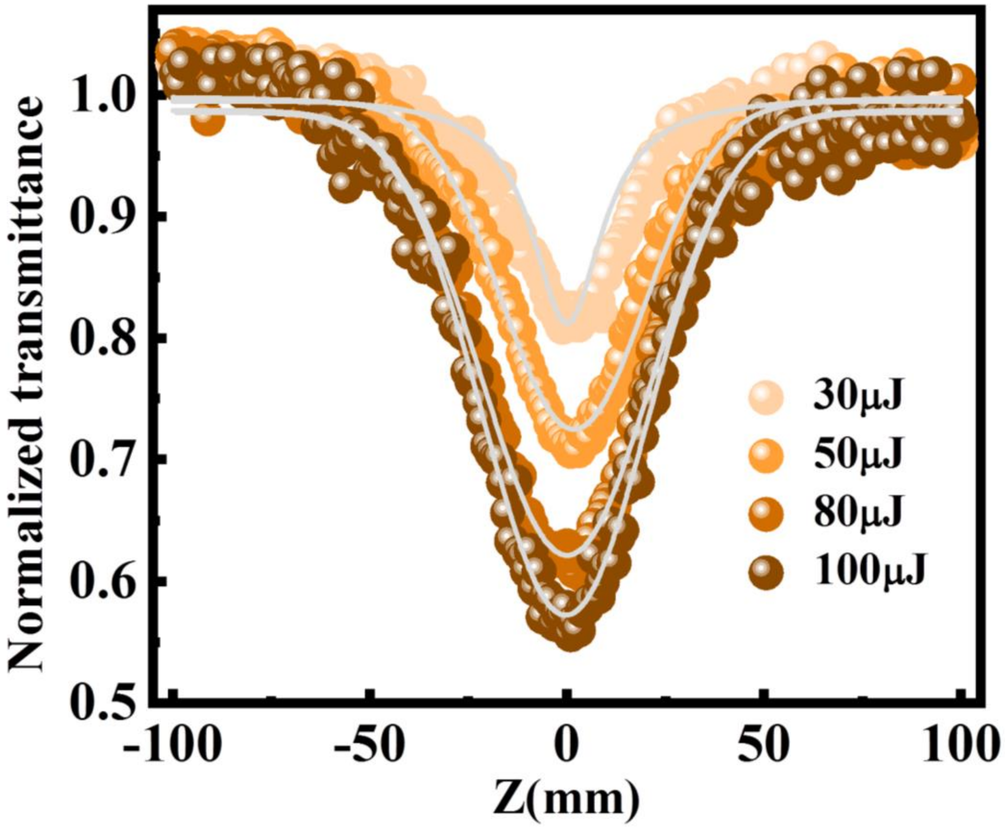

Figure S18. The NLO behavior of the C_{60}@PIZA-1 thin film at the different incident pulse energy.

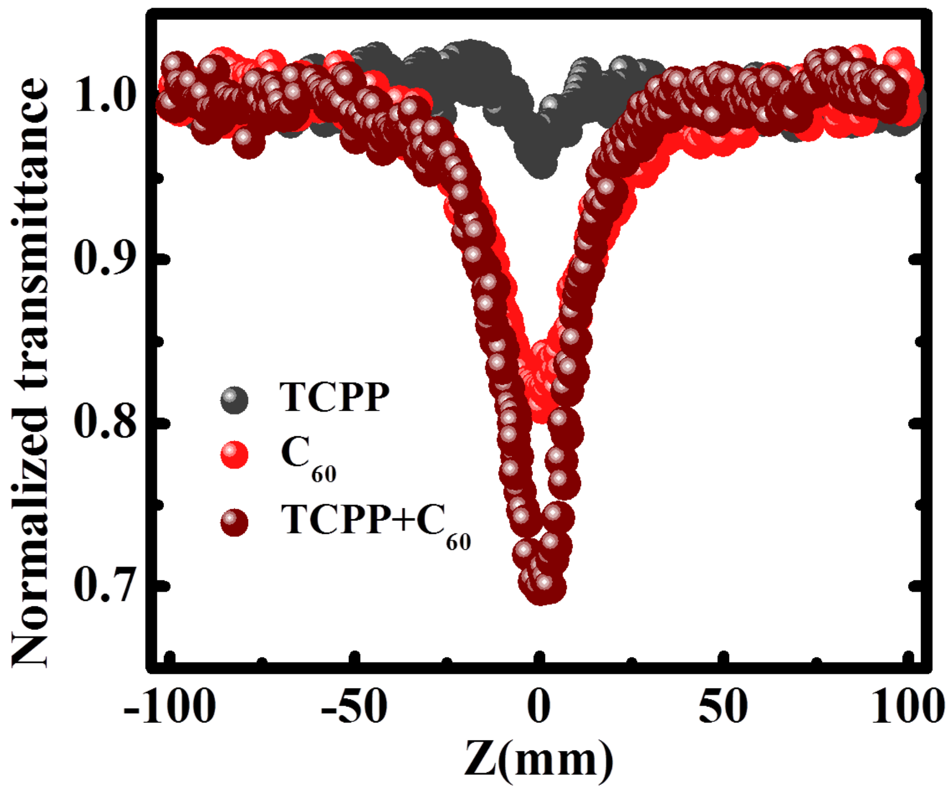

Figure S19. The NLO behavior of the porphyrin ligand, C_{60} and porphyrin ligand mixed with C_{60} film on quartz glass at 100 μJ .

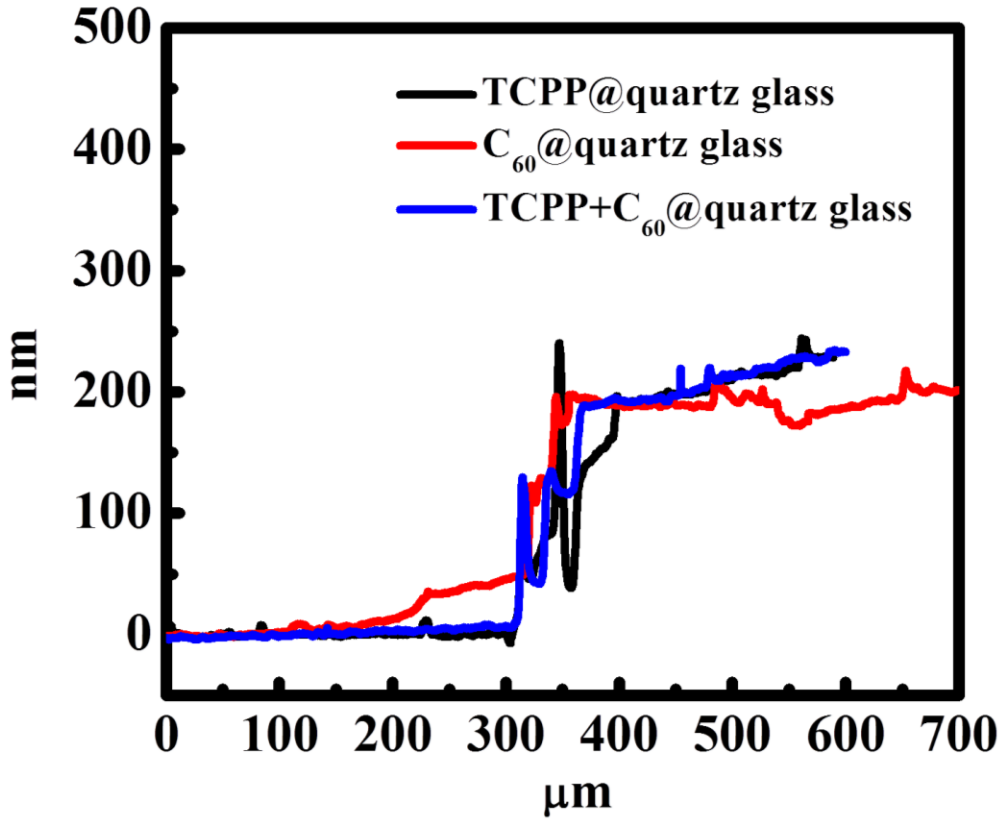

Figure S20. The thicknesses of porphyrin ligand, C_{60} and the porphyrin ligand mixed with C_{60} film on quartz glass.

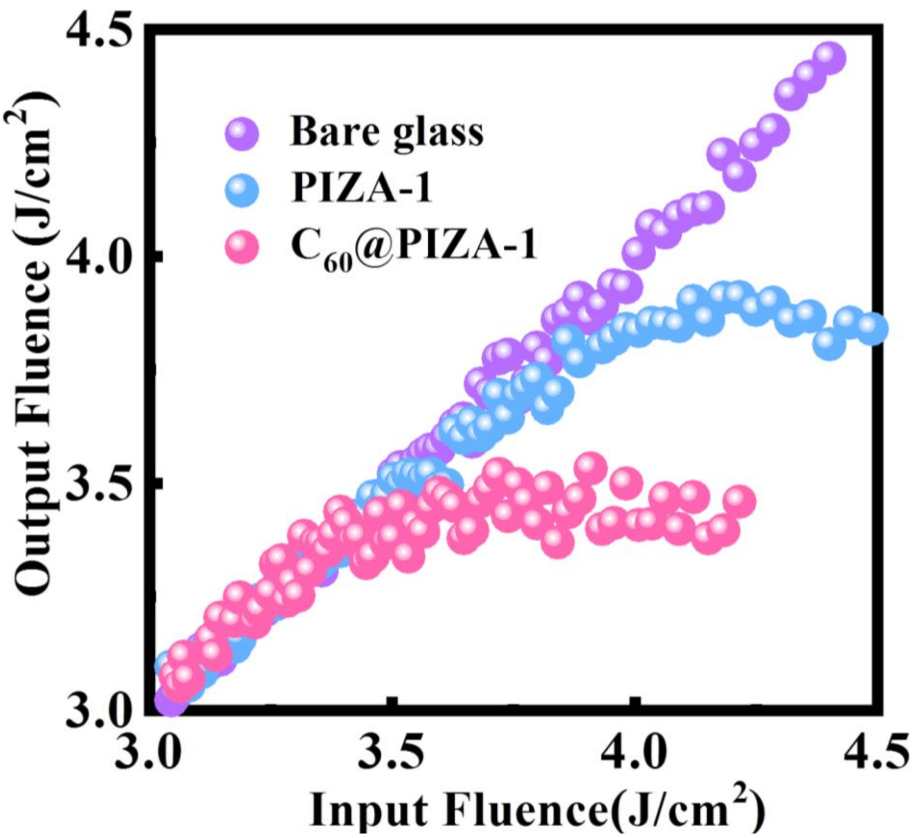

Figure S21. The curves of output fluence versus input fluence for bare glass, PIZA-1 thin film and C_{60}@PIZA-1 thin film.

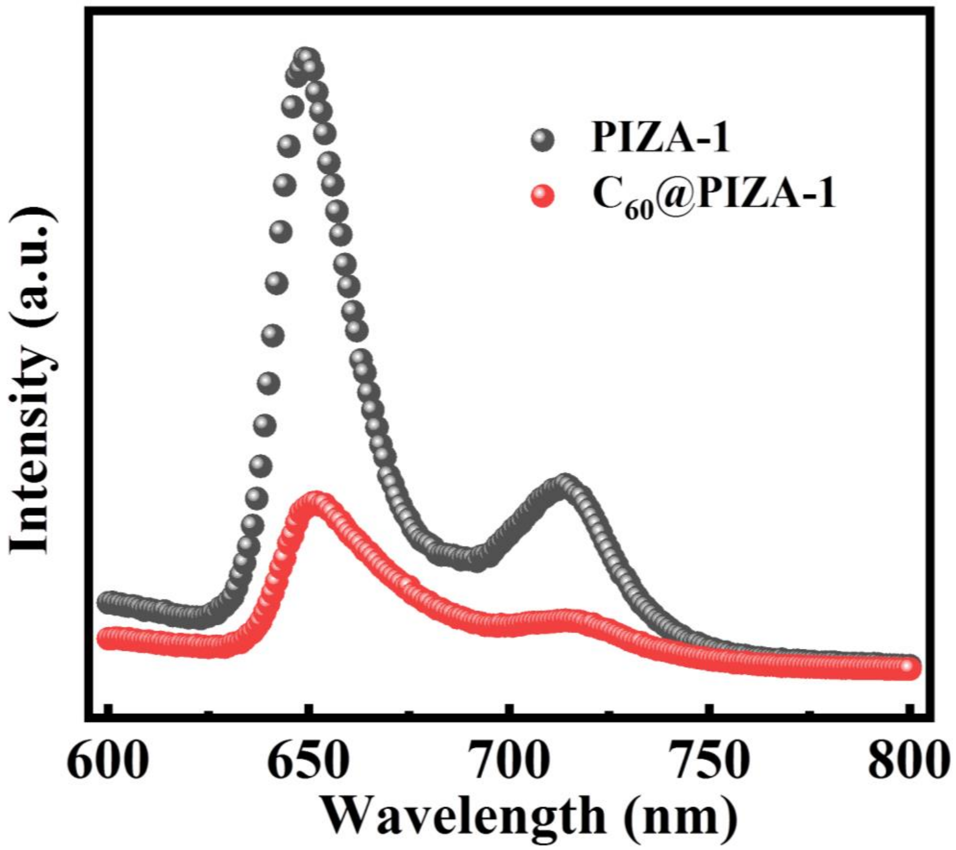

Figure S22. The fluorescence spectra of PIZA-1 and C_{60}@PIZA-1 thin film.

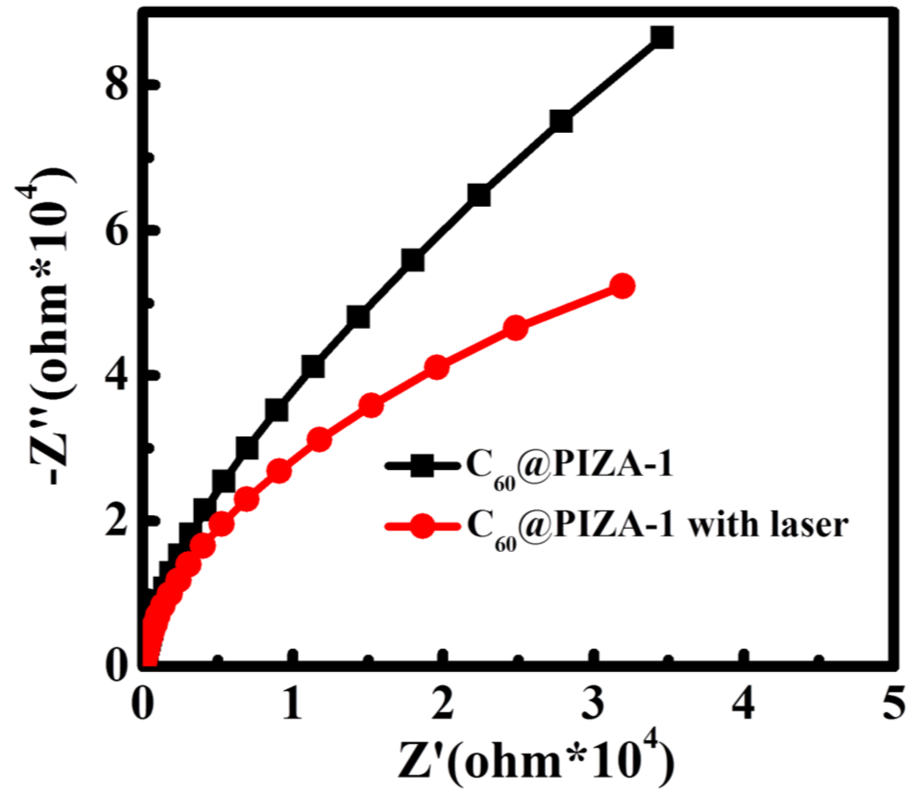

Figure S23. The EIS curves of C_{60}@PIZA-1 thin film with and without laser irradiation.

Table S2. Comparison of band gap of porphyrin-fullerene systems

Material	LUMO level	HOMO level	Band gap	Reference
$(Si\text{-}TCP)_n\text{-}PhC_{60}NH_3^+$	-3.87 eV	-5.45 eV	1.58 eV	1
$ZnP–Ph–C_{60}$	-3.36 eV	-5.17 eV	1.81 eV	2
$ZnP–EDOTV–C_{60}$	-3.34 eV	-5.05 eV	1.71 eV	2
$H_2P\text{-}C_{60}$	--	--	1.91 eV	3
$ZnP\text{-}C_{60}$	--	--	2.09 eV	3
C_{60}@PIZA-1	--	--	~1.69 eV	This work

1 P. Zhu, F. Song, P. Ma, S. Li and Y. Wang, *Dyes Pigments*, 2018, **151**, 385-390.

2 B. Pelado, F. Abou-Chahine, J. Calbo, R. Caballero, P. de la Cruz, J. M. Junquera-Hernandez, E. Orti, N. V. Tkachenko and F. Langa, *Chem. Eur. J.*, 2015, **21**, 5814-5825.

3 M.-L. Yu, S.-M. Wang, K. Feng, T. Khoury, M. J. Crossley, F. Yang, J.-P. Zhang, C.-H. Tung and L.-Z. Wu, *J. Phys. Chem. C*, 2011, **115**, 23634-23641.